Available online at www.sciencedirect.com
ScienceDirect
Ceramics International 38S (2012) S17–S20
CERAMICS INTERNATIONAL
www.elsevier.com/locate/ceramint

Phase formation and transitions in the lead nickel niobate–lead zirconate titanate system

Orawan Khamman [a,*], Rattikorn Yimnirun [b], Narin Sirikulrat [a], Supon Ananta [a]

[a] Department of Physics and Materials Science, Faculty of Science, Chiang Mai University, Chiang Mai 50200, Thailand
[b] School of Physics, Institute of Science, Suranaree University of Technology, and Synchrotron Light Research Institute, Nakhon Ratchsima 30000, Thailand

Available online 30 April 2011

Abstract

Despite the many previous studies of the synthesis and characterization of several perovskite ferroelectric materials which have potential applications in electronic and medical diagnostic devices, the synthesis and phase formation of the whole series in the solid solution of $(1-x)Pb(Ni_{1/3}Nb_{2/3})O_3$–$xPb(Zr_{1/2}Ti_{1/2})O_3$ (PNN–PZT) system has rarely been studied. In this work, the phase formation, morphology, particle size and chemical composition of perovskite powders in the $(1-x)$PNN–xPZT system were investigated. Powders were prepared by a modified mixed-oxide synthesis route for various chemical compositions under different calcination temperatures. It is found that the perovskite phase undergoes a pseudo-cubic to tetragonal transition as composition changes. The degree of spherical shape and agglomeration were observed to increase with increasing PZT content.

Keywords: A. Calcination; A. Powders: solid state reaction; B. X-ray methods; D. Perovskites

1. Introduction

The development of electroceramic materials especially the complex perovskite ceramics with high performance for such applications as transducers, sensors and nanoscale microprocessors has generated a great deal of interest among scientists [1,2]. Among the complex perovskite ferroelectrics, lead zirconate titanate (Pb(Zr, Ti)O_3 or PZT) and lead nickel niobate ($Pb(Ni_{1/3}Nb_{2/3})O_3$) or PNN) have been investigated extensively, both from academic and commercial viewpoints. Both materials are probably best known for their ferroelectric, piezoelectric and dielectric properties [1]. With their complimentary characteristics, it is expected that excellent properties can be obtained from ceramic in PNN–PZT system. It is well documented that the solid-solution of PNN with PZT is also a relaxor-type ferroelectric, which has drawn much interest in recent years for its excellent dielectric, especially electrostrictive properties [1,2].

Although many previous studies of the synthesis and characterization of these perovskite ferroelectric materials [1–3] have reported, however, the synthesis and phase formation of the whole series of the solid solutions in the PNN–PZT system has rarely been studied. Systematic investigation of these materials is required for a better understanding of the phase development in $(1-x)$PNN–xPZT solid solutions.

In this study, a frame work of compositions in the PNN–PZT systems will be developed based on the phase formation and morphology of the $(1-x)$PNN–xPZT powders. The phase formation characteristics of $(1-x)$PNN–xPZT powders were examined as a function of calcination conditions. The correlation between their compositions, phase formation and morphology of powders will be studied and discussed.

2. Experimental

The compositions of $(1-x)Pb(Ni_{1/3}Nb_{2/3})O_3$–$xPb(Zr_{1/2}Ti_{1/2})O_3$ were synthesized by the solid-state reaction of thoroughly ground mixtures of PNN and PZT powders that were milled in the required stoichiometric ratio. A vibratory laboratory mill (McCrone Micronizing Mill) was employed for preparing the powders. Polypropylene jar was used as a container and corundum balls were grinding media. The milling operation was carried out in isopropanol. A range of compositions based

* Corresponding author. Tel.: +66 53 94 3367; fax: +66 53 94 3445.
E-mail address: Orawankhamman@yahoo.com (O. Khamman).

0272-8842/$36.00
doi:10.1016/j.ceramint.2011.04.039

on the general formula $(1-x)$PNN–xPZT was prepared with values of x ranging from 0.0 to 1.0 at regular steps of 0.1. The raw materials were PbO, NiO, Nb_2O_5, ZrO_2 and TiO_2.

First, an intermediate phase of $NiNb_2O_6$ was prepared by the solid-state reaction method. The appropriate amount of PbO was then added to the $NiNb_2O_6$, vibro-milled and calcined in alumina crucible. Mixture was then calcined at 950 °C for 2 h. For the preparation of the PZT powders, the mixed-oxide method was used for preparation of PZT powders. In the first stage, PbO was reacted with ZrO_2 to give $PbZrO_3$, and in the second stage, TiO_2 and excess PbO were reacted with the $PbZrO_3$ to give the final product of PZT. PNN powders and PZT powders were used as starting materials for preparing $(1-x)$PNN–xPZT powders for solid solution. Each composition was calcined in air for 2 h at 900–1000 °C. $(1-x)$PNN–xPZT powders were examined by X-ray diffraction (XRD; Siemen-D500 diffractometer). The optimum calcination temperature of each composition was identified according to the minimum temperature required for the highest yield of perovskite [3]. Powder morphologies and particle sizes were directly imaged, using scanning electron microscopy (SEM; JEOL JSM-840A). The chemical compositions of the phase formed were elucidated by an energy-dispersive X-ray (EDX) analyzer with an ultra-thin window.

3. Results and discussion

Even though there have been many previous publications devoted to the characterization of PNN–PZT ceramics [4,5], no investigation has been made of the PNN–PZT solid solutions prepared using $NiNb_2O_6$ and $PbZrO_3$ key precursors. Thus, in this work, it is appropriated to examine the phase formation characteristics of these materials as a function of calcination conditions. The system under investigation is $(1-x)$PNN–xPZT, where x changed from 0.0 to 1.0 at regular intervals of 0.1. XRD patterns of all $(1-x)$PNN–xPZT powders calcined at their optimum conditions [5,6] are shown in Fig. 1. Here, it is seen that minor amounts of the $Pb_{1.45}Nb_2O_{6.26}$ (◆) have been found only at $x = 0.1$ and could be attributed to the effect of poor mechanical mixing and PbO volatilization [7], which was different from many previous work [4,5,8] where secondary or pyrochlore phases, such as $ZrTiO_4$, $Ti(Ni_{1/3}Nb_{2/3})O_4$ and $PbZrO_3$ were found. However, in the other compositions, it is seen that the $(1-x)$PNN–xPZT system formed a series of continuous solid solution of perovskite structure without any trace of pyrochlore phases. This observation indicates that the use of high purity PNN and PZT precursors at optimum calcination temperatures can effectively enhance the yield of the perovskite phase without any addition of excess PbO. For $x = 0$ (pure PNN), the X-ray diffraction pattern shows only one (2 0 0) sharp peak (Fig. 2) confirming its (pseudo) cubic symmetry, in good agreement with literatures [6,7]. By increasing the PZT content, the intensity ratios of the (0 0 2)/(2 0 0) peaks tend to increase up to $x = 0.8$, where both the tetragonal and rhombohedral (2 0 0) peaks were found. The X-ray diffraction patterns of powders with high PZT content ($x > 0.8$) showed in all cases the co-existence of both rhombohedral (R) and tetragonal (T) phases, which are characterized by (0 0 2)T, (2 0 0)R and (2 0 0)T peaks splitting the diffraction line around 2θ of 43–46° (Fig. 2), consistent with those found for the perovskite PZT-BT system [3].

The variation of these triplet-diffraction lines as a function of PZT content could be explained by microscopic compositional fluctuations occurring in these perovskite materials, which cannot provide real homogeneity in the solid solutions, and also by the different stresses induced in the particles, which determine the co-existence of tetragonal–rhombohedral (and probably-cubic) phases [6]. Robert et al. [5] reported that the $(1-x)$PNN–xPZT system undergoes a cubic to (pseudo) cubic phase transformation, followed by a (pseudo) cubic to tetragonal and rhombohedral transition, respectively at $x \sim 0.6$. While Vittayakorn et al. [6] argued that the MPB of the solid solution $(1-x)$PNN–xPZT (Zr/Ti = 50/50) is located at $x \sim 0.8$.

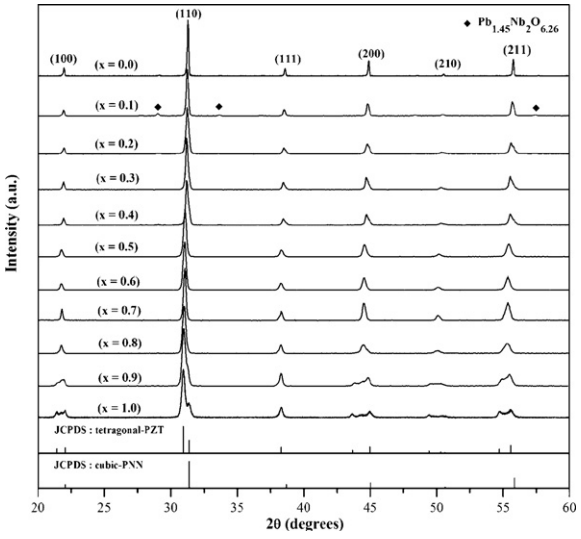

Fig. 1. XRD patterns of the $(1-x)$PNN–xPZT powders after calcined at their optimum conditions.

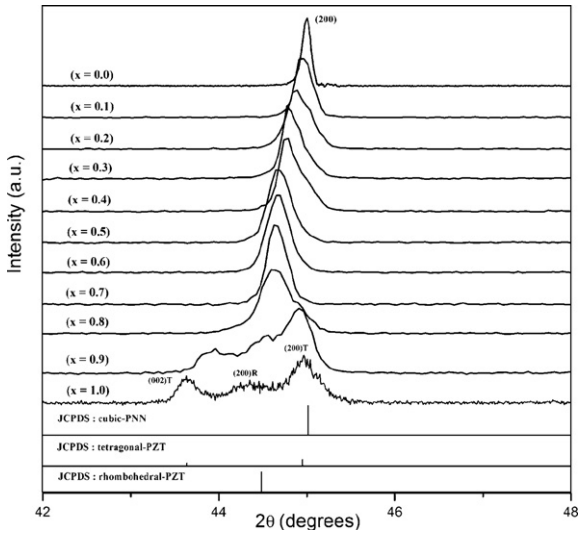

Fig. 2. Enlarged XRD patterns of the $(1-x)$PNN–xPZT powders, showing triplets (0 0 2)T, (2 0 0)R and (2 0 0)T.

However, in the present study, the composition boundary between the real tetragonal, rhombohedral and (pseudo) cubic phases could not be delimited under the present experimental limit of accuracy. Two possible ranges of compositions for further studies are $0.8 < x < 0.9$ and $0.0 < x < 0.1$. High resolution XRD analysis is necessary to detect the possible superposition of phases and to restrict the range of compositions for better characterization of the $(1 - x)$PNN–xPZT compositions in the range of structural change. Optimum calcination temperature which is the minimum firing temperature required to achieve a single-phase perovskite powder for each PZT is demonstrated in Fig. 3. It is seen that by increasing PZT content, the optimum firing temperature for highest perovskite phase formation tend to decrease. These observations can be attributed to the lower optimized calcination temperature of PZT (∼900 °C), when compared with PNN (∼1000 °C). The optimum calcination temperatures observed in this work are in the range similar with those reported earlier [6,8].

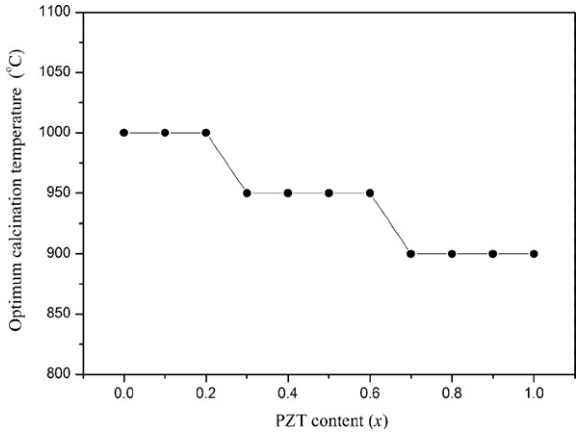

Fig. 3. Variation of the optimum calcination temperature as a function of PZT content.

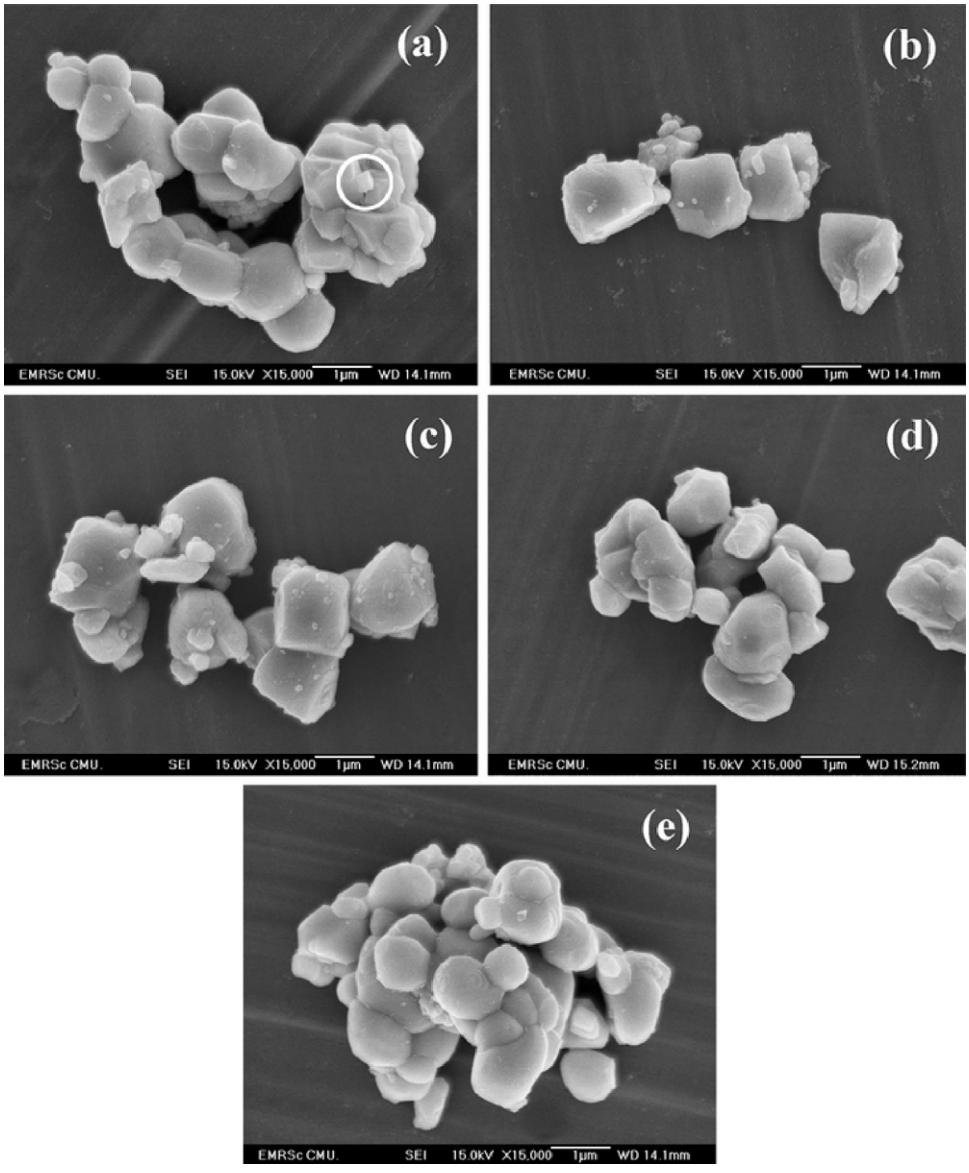

Fig. 4. SEM micrographs of the calcined $(1 - x)$PNN–xPZT powders with x = (a) 0.1, (b) 0.3, (c) 0.5, (d) 0.7 and (e) 0.9.

Table 1
Particle size of $(1-x)$PNN–xPZT powders calcined at their optimum conditions.

Powders	Particle size (μm)
0.9PNN–0.1PZT	0.67–1.48
0.7PNN–0.3PZT	0.40–1.34
0.5PNN–0.5PZT	0.48–1.40
0.3PNN–0.7PZT	0.61–1.24
0.1PNN–0.9PZT	0.45–1.18

Table 2
Chemical compositions of the calcined $(1-x)$PNN – xPZT powders from EDX analysis.

Compositions (at%)					Possible phases
Pb(M)	Zr(L)	Ti(K)	Ni(K)	Nb(L)	
13.55	0.57	0.45	4.33	15.14	0.9PNN–0.1PZT
14.04	2.32	2.68	3.78	10.43	0.7PNN–0.3PZT
15.09	4.51	3.79	2.64	6.01	0.5PNN–0.5PZT
13.04	3.08	4.39	1.67	3.25	0.3PNN–0.7PZT
16.02	7.29	8.74	0.65	2.13	0.1PNN–0.9PZT

SEM micrographs of the $(1-x)$PNN–xPZT powders are shown in Fig. 4(a)–(e), indicating representative morphologies. These samples are calcined at their optimum temperatures. In general, similar morphological characteristics were observed in these powders, *i.e.* agglomerated and basically irregular in shape, with a substantial variation in particle size. The results indicate that the degree of agglomeration tend to increase with increasing PZT content. For $x = 0.1$, it was found that $(1-x)$PNN–xPZT particles which have an angular morphology, coexist with some small particles (circled in Fig. 4(a)). The small particle was confirmed as pyrochlore phase ($Pb_{1.45}Nb_2O_{6.26}$) by EDX analysis, which is in good agreement with XRD results.

The particle sizes of PNN–PZT powders calcined at various ratios are also listed in Table 1. These results indicate that the particle sizes were estimated to be around 0.40–1.48 μm, similar with other work [8]. In addition, these powders tended to form agglomerates of the fine particles. It is believed to calcine at lower temperature. At $x = 0.9$, the powders showed similar morphologies which have a spherical shape and good homogeneity. In this study, it is clear that all powders exhibit a higher significant level of spherical shape and agglomeration with increasing PZT content.

Corresponding EDX analysis and chemical compositions for some of these $(1-x)$PNN–xPZT powders are shown in Table 2. It can be seen that the $(1-x)$PNN–xPZT powders with different compositions are composed of a variation in Pb/Zr/Ti/Ni/Nb ratios. In addition, the Zr and Ti concentration increases with increasing PZT content. The combination of X-ray and SEM/EDX results strongly support that in this study, the series of $(1-x)$PNN–xPZT solid solution were formed.

4. Conclusions

The perovskite powders in the $(1-x)$PNN–xPZT system were successfully processes by employing $NiNb_2O_6$ and $PbZrO_3$ precursors. This study has demonstrated the phase formation and transition mechanism of perovskite powders in the $(1-x)$PNN–xPZT system. X-ray diffraction has indicated that complete solid solution occurs across the entire compositional range of $(1-x)$PNN–xPZT the system. In composition range for a stable perovskite structure, the composition boundary between the tetragonal, rhombohedral and cubic phases is identified at $x = 0.1$, 0.8 and 0.9, respectively. It is seen that by increasing PZT content, a level of spherical shape and agglomeration increased while optimum calcination temperatures decreased.

Acknowledgements

This work was supported by the Thailand Research Fund (TRF), the Commission on Higher Education (CHE), and Faculty of Science, Chiang Mai University.

References

[1] A.J. Moulson, J.M. Herbert, Electroceramics: Materials, Properties, Applications, 2nd ed., John Wiley & Sons Ltd., 2003.
[2] G.H. Haertling, Ferroelectric ceramics: history and technology, Journal of the American Ceramic Society 82 (1999) 797–818.
[3] W. Chaisan, S. Ananta, T. Tunkasiri, Synthesis of barium titanate–lead zirconate titanate solid solutions by a modified mixed-oxide synthetic route, Current Applied Physics 4 (2–4) (2004) 182–185.
[4] E.F. Alberta, A.S. Bhalla, Piezoelectric and dielectric properties of transparent $Pb(Ni_{1/3}Nb_{2/3})_{1-x-y}Zr_xTi_yO_3$ ceramics prepared by hot isostatic pressing, International Journal of Inorganic Materials 3 (2001) 987–995.
[5] G. Robert, M.D. Maeder, D. Damjanovic, N. Setter, Synthesis of lead nickel niobate–lead zirconate titanate solid solutions by a *B*-site precursor method, Journal of the American Ceramic Society 84 (2001) 2869–2872.
[6] N. Vittayakorn, G. Rujijanagul, X. Tan, M.A. Marquardt, D.P. Cann, The morphotropic phase boundary and dielectric properties of the $xPb(Zr_{1/2}Ti_{1/2})O_3$–$(1-x)Pb(Ni_{1/3}Nb_{2/3})O_3$ perovskite solid solution, Journal of Applied Physics 96 (2004) 5103–5109.
[7] C.H. Lu, W.J. Hwang, Preparation of $Pb(Zr,Ti)O_3$-$Pb(Ni_{1/3}Nb_{2/3})O_3$ solid solution powder from hydrothermally-treated precursors, Materials Letters 27 (1996) 229–232.
[8] A.L. Costa, C. Galassi, G. Fabbri, E. Roncari, C. Capiani, Pyrochlore phase and microstructure development in lead magnesium niobate materials, Journal of the European Ceramic Society 21 (2001) 1165–1170.